Journal of Power Sources 196 (2011) 1078–1083

Contents lists available at ScienceDirect

Journal of Power Sources

journal homepage: www.elsevier.com/locate/jpowsour

Study of core–shell platinum-based catalyst for methanol and ethylene glycol oxidation

D. Kaplan[a], M. Alon[a], L. Burstein[b], Yu. Rosenberg[b], E. Peled[a,*]

[a] School of Chemistry, Tel Aviv University, Tel Aviv 69978, Israel
[b] Wolfson Applied Materials Research Center, Tel Aviv University, Tel Aviv 69978, Israel

ARTICLE INFO

Article history:
Received 6 May 2010
Received in revised form 19 July 2010
Accepted 10 August 2010
Available online 17 August 2010

Keywords:
Core–shell
Platinum
Catalyst
Methanol
Ethylene glycol
Oxidation

ABSTRACT

A Ru_{core}–Pt_{shell}, XC72-supported catalyst was synthesized in a two-step process: first, by deposition of Ru on XC72 by the polyol process and then by deposition of Pt on the XC72-supported Ru, with $NaBH_4$ as reducing agent. The structure and composition of this core–shell catalyst were determined by EDS, XPS, TEM and XRD. Electrochemical characterization was determined with the use of cyclic voltammetry and chronoamperometry. The methanol and ethylene glycol oxidation activities of the core–shell catalyst were studied at 80 °C and compared to those of a commercial catalyst. It was found to be significantly better (in terms of A g^{-1} of Pt) in the case of methanol oxidation and worse in the case of ethylene glycol oxidation. Possible reasons for the lower ethylene glycol oxidation activity of the core–shell catalyst are discussed.

1. Introduction

Alternative sources of energy that are efficient, renewable and environmentally friendly remain one of the biggest challenges for the scientific and industrial community. Fuel cells are a potential answer to that challenge [1]. A promising type of fuel cell is the direct methanol fuel cell (DMFC).

While methanol has better handling properties than hydrogen, since it is liquid at room temperature, it is still poisonous to some extent and also flammable. In addition, when used in PEM-based fuel cells, methanol has a tendency to cross over through the membrane from anode to cathode, thus poisoning the cathode catalyst. Ethylene glycol (EG) may be a successful replacement for methanol, since it has a much higher boiling point than methanol (198 °C vs. 64.7 °C) and greater volumetric capacity (4.8 Ah ml^{-1} vs. 4.0 Ah ml^{-1}) [2]. Moreover, since EG is a much larger molecule, fuel crossover to the cathode can be much lower. Until now, several studies of EG as a potential fuel in acidic media, have been conducted [2–7]. One of the handicaps preventing DMFCs from becoming widespread commercial product is the high Pt loading in the electrodes used in DMFC which leads to high costs of the DMFC.

The catalytic process in the case of bimetallic Pt–Ru occurs on two different sites on the surface of the catalyst. Platinum sites break down the fuel molecules (methanol or EG as the case may be) and this leads to the formation of CO species chemisorbed on the platinum sites. These adsorbed CO species are oxidized to CO_2 with the assistance of ruthenium surface sites that dissociate the adsorbed water molecules [8,9]. Since ruthenium is much cheaper than platinum, it is logical to try to reduce the amount of platinum in the catalyst, by using it only on the surface (as a monolayer) rather than in the bulk as well, thus greatly reducing the cost of the catalyst. There have been several reports in the literature on attempts to reduce the platinum loadings by the preparation of Ru_{core}–Pt_{shell} and platinum-decorated ruthenium catalysts. Some of the results obtained in these studies led to quite differing conclusions regarding the activity of Ru_{core}–Pt_{shell} catalysts vs. Pt–Ru alloy catalysts [8,10,11].

In a search for active, low cost and stable catalysts we have synthesized and characterized a carbon-supported Ru_{core}–Pt_{shell} catalyst with 44% (w/w) total metal. The catalyst powder was characterized by EDS, XRD, TEM and XPS. Catalyst ink-based electrodes were characterized by XPS and cyclic voltammetry. The methanol and EG oxidation activity of both synthesized and commercial (Johnson Matthey HiSPEC7000) catalysts were studied with the use of CV in sulfuric acid solutions containing methanol or EG. In addition, preliminary experiments on the stability of both catalysts were performed.

* Corresponding author. Tel.: +972 3 6408438; fax: +972 3 6414126.
E-mail address: peled@post.tau.ac.il (E. Peled).

0378-7753/$ – see front matter © 2010 Elsevier B.V. All rights reserved.
doi:10.1016/j.jpowsour.2010.08.022

2. Experimental

2.1. Catalyst preparation

500 mg of Vulcan XC72 (BET specific surface area of 272 $m^2\,g^{-1}$) decorated with 1% (w/w) of platinum was prepared by an electroless deposition process with $NaBH_4$ as the reducing agent. XC72 was added to a solution of 0.4 M HCl + $PtCl_4$ and the mixture was stirred for 2 h. At this point 32% ammonia was added in several 2 ml portions, while the mixture was stirred, in order to reach a pH ≈ 11. An excess of $NaBH_4$ was dissolved in about 10 ml H_2O and this was rapidly added to the mixture, which was then stirred for another 2 h. It was assumed that at this point, all the metal ions in the solution had been reduced by $NaBH_4$ and deposited on the carbon. The powder obtained was recovered by centrifugation, washed with distilled water until no chloride ions could be detected, and dried by evaporation. The purpose of the deposited 1% platinum was to enable easier deposition and smaller particle size of ruthenium on XC72 during the next stage [12].

Ruthenium was deposited on the 1%Pt/XC72 with the use of the polyol process, by a procedure similar to that described in [13]. 1 g of $RuCl_3{\cdot}H_2O$ (Sigma Aldrich) and the abovementioned powder were dissolved in 900 ml of EG, sonicated for 2 h and refluxed at 170 °C for 3 h. The resulting mixture was filtered through a Buchner funnel and washed with deionized water and acetone. The resulting powder was dried in a vacuum oven at 100 °C for 12 h.

A Pt/Ru/XC72 catalytic powder was obtained from Ru/XC72 with the use of the electroless deposition process described above, with $NaBH_4$ as the reducing agent.

Finally, the powder was treated in 1 M H_2SO_4 at 80 °C for 8 h in order to obtain a stable catalyst with Ru_{core}–Pt_{shell} structure.

2.2. Catalyst characterization

X-ray diffraction (XRD) data were collected with Cu Kα radiation on Θ–Θ powder diffractometer Scintag equipped with a liquid nitrogen cooled Ge solid-state detector. XRD patterns were treated by JADE 9.1+ software [14] including whole pattern fitting (WPF)/Rietveld refinement facilities with structure information available from ICDD [15] and ICSD [16] databases.

XPS measurements were performed with the use of a 5600 Multi-Technique System (PHI, USA). The samples were irradiated with an Al Kα monochromated source (1486.6 eV) and the emitted electrons were analyzed by a Spherical Capacitor Analyzer with a slit aperture of 0.8 mm They were analyzed at the surface and after sputter cleaning with the 4 kV Ar^+ Ion Gun, at a sputter rate of 39 Å min^{-1} on reference SiO_2/Si sample. High-resolution measurements were performed with pass energy of 11.75 eV.

The dispersion of the homemade catalyst on support and its local composition were investigated by transmission electron microscopy (TEM) on a Tecnai F20 (FEI) with a 200 kV field emission gun. The powder samples were sonicated in ethanol and put on 200 square mesh copper grids with carbon film (CF200-Cu, by Electron Microscopy Sciences). The local composition of the nanoparticles was examined by placing the EDS probe on the edge and the middle parts of the nanoparticles.

A JOEL (JSM-6300) scanning electron microscope, made by JOEL (JSM-6300), with X-Ray LINK detector and Pentafen window was used for EDS measurements. The software used for element recognition, was LINK ISIS.

2.3. Electrode preparation and characterization

Cyclic voltammetry and chronoamperometry tests were performed in a three-compartment glass cell, with an Ag/AgCl/3 M KCl reference electrode in a Luggin capillary compartment and a palladium wire counter electrode. All potentials in this paper are converted to the reversible-hydrogen-electrode (RHE) scale. The working electrode holder was a 1 cm × 5 cm glassy-carbon rectangle. Carbon-supported catalysts (both homemade Pt/Ru/XC72 and commercial JM) were applied to the lower part of this rectangle by transferring 10 μl of a sonicated catalyst ink. This ink consisted of 10 mg catalyst powder, 56.6 μl (55.3 μl for JM), 5% (w/w) Nafion solution, 3 g H_2O and 2 g ethanol. All electrochemical experiments were carried out at 80 °C with the use of an Eco Chemie (Netherlands) AUTOLAB potentiostat.

A study of the electrochemically active surface area (ECSA) was carried out in a quiescent 0.5 M H_2SO_4 solution. Nitrogen was bubbled through the solution for 15 min before the measurement and passed over the solution during the voltage scan. The cell was cycled between 0 and 1.2 V at a sweep rate of 20 mV s^{-1}, for a total of 10 scans. The electrochemical surface area of platinum and ruthenium was determined from the coulometric charge in the hydrogen-desorption region, under the assumption of 210 μC cm^{-2} of hydrogen adsorbed [2,17,18]. All values of ECSA are normalized to both platinum loading [$m^2\,g^{-1}$(Pt)] and to total metal loading [$m^2\,g^{-1}$(Pt–Ru)]. The question is, which way of ECSA calculation, normalized to Pt weight or to total metals weight (Pt + Ru), better reflects the catalyst properties in this work? As we do not have a precise answer, we have presented both values. However, we found (unpublished results) that under our cycling conditions (0–1.2 V, at 80 °C), Ru/XC72 is virtually inactive in the hydrogen (RuH) region, probably as a result of extensive, irreversible ruthenium oxide formation. This extremely low activity of ruthenium under our experimental conditions, leads us to believe that ECSA values normalized to platinum loading better represent the actual electrochemically active surface area of the catalysts.

It was previously shown that the use of the hydrogen-desorption region in the determination of ECSA for Ru and Pt–Ru alloy is problematic because of the overlap of the hydrogen and ruthenium oxidation currents [17,18]. However, it can be seen in Fig. 2, that for the homemade catalyst, the first peak (labeled as peak 1) of the ruthenium oxidation is very small compared to the hydrogen-desorption peak. The same peak for the commercial (Pt–Ru alloy) catalyst is virtually non-existent. This leads us to the assumption that the additional charge due to ruthenium oxidation is very small.

Since our main goal in the article is not to report a high precision ECSA measurement of the Pt–Ru-based catalyst, but its activity towards fuel oxidation, we believe that the ECSA values presented in the article are a good first-order approximation, and are suitable for the purpose of the article.

Studies of methanol and EG oxidation activity were carried out immediately after the ECSA tests. The experimental setup was the same but the solutions were 0.5 M H_2SO_4, 0.1 M MeOH and 0.5 M H_2SO_4 and 0.4 M EG, respectively. A total of 20 scans were performed for each fuel. EG oxidation was performed on the same electrodes, after initial ECSA studies, MeOH oxidation and additional ECSA studies were concluded. Following the completion of the fuel oxidation tests, additional ECSA measurements were performed.

Chronoamperometric studies of methanol oxidation were performed in the same experimental setup but with stirring by magnetic stirrer in the working electrode compartment. The stirring was intended to simulate a flow of electrolyte and fuel solution in a real fuel cell. The experiments were performed following a conditioning process, in which the electrode went through 20 scans in 0.5 M H_2SO_4, 20 scans in 0.5 M H_2SO_4, 0.1 M MeOH and an additional 20 scans in 0.5 M H_2SO_4. The voltage applied during chronoamperometry was 0.45 V (RHE) since this is approximately the operating voltage of the anode in DMFC operating at high current [19]. After every 600 s period of 0.45 V applied voltage, there was a period of 10 s during which 0 V was applied to the working

Table 1
Homemade Pt/Ru/XC72 catalyst-atomic ratios.

Metal	Nanopowder—XPS results		Ink—XPS results		Nanopowder EDS results
	Before sputtering	After 1.4 min sputtering	Before sputtering	After 1.5 min sputtering	
Ru	1	1	1	1	1
Pt	4.28	1.19	4.27	1	0.43

electrode. This mode of operation was previously found to allow better performance of DMFCs [3,19,20]. The total time frame of chronoamperometry was 3200 s.

3. Results and discussion

3.1. Physicochemical analysis

The XPS results can be seen in Table 1 and the spectrum is shown in Fig. 1a and b. For both the powder and the ink samples, the surface consists of over 80% platinum, with only 35% of it alloyed with Ru.

Deconvoluted XPS data for C1s and Ru3d (Fig. 1a) show that the Ru:RuO_2 ratio was ≈2.8. However, it must be remembered that this ratio was relevant to the specific conditions existing during the XPS examination, and can be significantly different during electrochemical analysis.

After only a short sputtering time (1.4 and 1.5 min) the ruthenium content increases to 45–50%. It can be seen in Fig. 1b, that after 1.5 min of sputtering, the platinum peaks were shifted to higher energies, which indicates, after comparison with the XPS results of the commercial catalyst (Fig. 1b), a larger presence of a Pt–Ru alloy below the surface (55% of the platinum was alloyed). This is important evidence that the platinum was deposited on ruthenium and not directly on the carbon particles.

XRD patterns of commercial JM and homemade Pt/Ru/XC72 catalysts are shown in Fig. 1c; the homemade pattern is depicted with offset for clarity. The lower pattern unambiguously demonstrates that the commercial sample has face centered cubic (FCC) structure; herewith its Bragg diffraction peaks are shifted to the higher angles from the positions of pure Pt reflections marked by sticks. This shift probably originates from Pt–Ru alloy formation when smaller Ru atoms with atomic radius 1.340 Å substitute accidentally in platinum FCC host bigger Pt atoms whose atomic radius is 1.387 Å.

Performing pattern decomposition by profiles fitting we could estimate positions and widths of individual peaks. Then from (1 1 1) Bragg reflection position we get corresponding lattice spacing 2.225 ± 003 Å vs. 2.265 Å of powder Pt standard, PDF card 4-802 [15]. Basing on validity of Vegard's law [21] in Pt–Ru system [22] we can evaluate composition of commercial JM sample as $Pt_{48.5}Ru_{51.5}$ which is very close to its certificate data. The mean size of coherent scattering domain ("grain size") estimated by Scherrer equation [23] from the corrected for instrumental broadening width of (1 1 1) reflection was found to be 2.1 ± 0.1 nm.

These results go well with that of quantitative analysis obtained for the same sample by WPF refinement for both concentrations of elements (33.5 wt.% of Pt, 16.5 wt.% of Ru and 50 wt.% of carbon) and Pt–Ru alloy's crystallite size (2.3 nm).

Judging by Fig. 1c, the structure and composition of the homemade catalyst differs essentially from the commercial JM one. Close inspection of the upper XRD pattern allows inferring that in addition to marked on the graph carbon, hexagonal Ru and tetragonal RuO_2 phases, homemade Pt/Ru/XC72 catalyst contains also Pt contribution—the most evident traces of FCC Pt presence can be seen near 40 and 82 degrees 2Θ.

It was found by WPF analysis that the homemade sample in addition to carbon contains following particles: 5.4 nm Ru (57.0 wt.%), 2.7 nm Pt (21.5 wt.%) and 10 nm RuO_2 (4.0 wt.%). Thereby Ru/Pt atomic ratio in the system is equal to 5.25 provided that we neglect small oxide fraction. At the same time the analogous ratio determined by EDS is 2.3 (1/0.43 = 2.3, see Table 1) which means that at least half of Pt atoms residing in the system do not take part in diffraction and are unseen in the XRD pattern.

In our opinion, this contradiction can be resolved by taking into account the catalyst's preparation process and the XPS results, and, assuming that deficient ("XRD-lost") Pt atoms are distributed over surfaces of Ru particles. Taking into account that in FCC Pt (FIZ#52250 [16]) and hexagonal Ru (FIZ#43710 [16]) mean atomic volumes are 15.0 and 13.5 $Å^3$, respectively, we easily obtain from XRD data that the number of Pt grains in the sample is about 1.6 times more than Ru ones, and the amount of "XRD-lost" Pt atoms is sufficient to form on an average ∼2 Å layer around Ru core.

It may seem that this Pt coating may look like monolayer Pt shell observed in Ru_{core}–Pt_{shell} nanoparticles [24], although in contrast to [24] where Ru cores were highly distorted, the long range order in our Ru cores provides well defined XRD pattern. A specific structural design of this shell is beyond the scope of our XRD analysis; for instance, the real Pt coating has not to be continuous but consisting of small Pt clusters or islets [25]. In fact, the electrochemical analysis discussed later, supports the small Pt islets structure.

TEM examination (Fig. 1d) showed a good dispersion of the metallic nanoparticles on the carbon support. In addition, examination of the local composition of the catalyst particles revealed that the atomic ratio Pt:Ru at the edges of the particles was ≈1.5, while the same atomic ratio in the particle centers was ≈0.5.

These physicochemical analyses reveal that, while the predominant metal in the catalyst is ruthenium (according to XRD and EDS), only the core is highly enriched with ruthenium while the shell is highly enriched with platinum, both in nano-powder and in ink (according to XPS and TEM). In fact, it proves that the homemade catalyst has the intended Ru_{core}–Pt_{shell} structure.

3.2. Electrochemical analysis

Voltammograms of both catalysts, obtained from ECSA studies in 0.5 M H_2SO_4 solution at 80 °C, can be seen in Fig. 2. In the anodic sweep of the voltammogram of the homemade catalyst, there are two distinguishable peaks (marked 1 and 2). Peak 1 is characteristic of the ruthenium oxidation process while peak 2 is characteristic of platinum oxidation. Neither peak is seen in the voltammogram of the JM catalyst. There is also a fundamental difference between the responses of the catalysts in the cathodic sweep. In case of the JM catalyst, there is a minimum at 0.45 V, characteristic of the reduction of the Pt–Ru alloy oxide [26]. The homemade catalyst exhibits a drastically different shape in the cathodic direction. There is no minimum at 0.45 V, but there are two minima: at 0.8 V (peak 3) and 0.25 V (peak 4). These are characteristic of the reduction of platinum oxide and ruthenium oxide, respectively [26]. This is yet another proof that our homemade Pt/Ru/XC72 catalyst is fundamentally different from the commercial JM Pt–Ru alloy-based catalyst. The surface of our catalyst is not a solid solution of Pt–Ru, but rather both elements remain as separate phases.

As ruthenium is more than an order of magnitude cheaper than platinum, the ECSA values and the oxidation current of methanol and EG were normalized to the mass of platinum. The ECSA val-

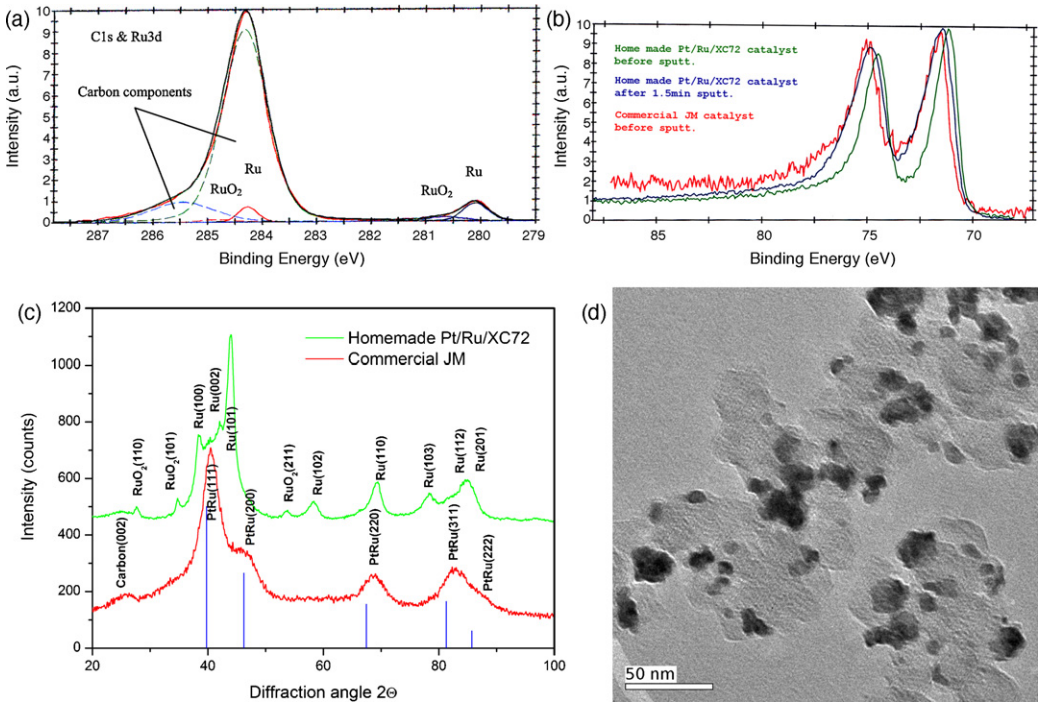

Fig. 1. (a) Homemade Pt/Ru/XC72 catalyst ink, normalized XPS spectra (C1s and Ru3d region, including deconvolution). (b) Homemade Pt/Ru/XC72 and commercial JM catalysts, normalized XPS spectra (Pt 4f region). (c) XRD patterns of commercial JM and homemade Pt/Ru/XC72 catalysts. (d) TEM image of the homemade Pt/Ru/XC72 catalyst.

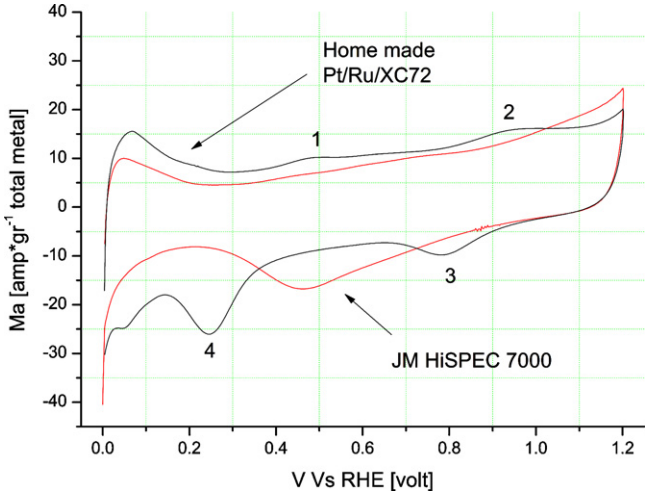

Fig. 2. Typical voltammograms of ECSA studies in 0.5 M H_2SO_4 solution, scan rate: 20 mV s^{-1}.

ues (normalized to platinum loading, see Table 2), were 42 and 25 ($m^2\,g^{-1}$ Pt) for homemade and JM catalysts, respectively. This is not surprising if one takes into account the low total amount of platinum that is present only in the shell of the particles of the homemade catalyst.

Voltammograms showing catalyst activity for the oxidation of methanol and EG can be seen in Fig. 3a and b. For comparison between the two catalysts in question, a value of the current (normalized to the total amount of platinum in the catalysts) at 0.45 V was taken. As can be seen from Fig. 3a and Table 2, the Pt/Ru/XC72 catalyst is clearly superior to the JM catalyst for methanol oxidation. The values obtained from the voltammograms are 471 A g^{-1} Pt in the case of the Pt/Ru/XC72 catalyst and 346 A g^{-1} Pt in the case of the JM catalyst. This translates to a 36% improvement in methanol oxidation activity for every gram of platinum.

The XPS and the CV of the catalyst (Fig. 2) indicate the coexistence of platinum and ruthenium atoms on the surface (shell) of the homemade catalyst particles. Moreover, the XPS results showed only 35% of alloy formation in the shell itself vs. 55% after sputtering. These results indicate the presence of a Pt–Ru alloy-like interphase layer between the shell and the core. When normalizing the $I_{0.45\,V}$ values to the ECSA of the samples (normalized to platinum loading, see Table 2) we find that the JM catalyst made of Pt–Ru alloy is more active than the core–shell catalyst. This leads to the conclusion that the Pt–Ru surface alloy (JM) is more active than a mosaic of platinum and ruthenium particles in the shell. So it may be beneficial to study a Pt–Ru particle shell on a ruthenium core. The superior oxidation activity per gram of platinum can be attributed to the low total amount of platinum in the catalyst, i.e., the Ru_{core}–Pt_{shell} catalyst utilizes platinum better than JM Pt–Ru catalyst.

The picture changes when looking at the EG oxidation voltammogram in Fig. 3b. In this case, the JM catalyst has the higher activity, although not by much: 263 A g^{-1} Pt vs. 241 A g^{-1} Pt. The reason for the superiority of the JM catalyst can be seen if we compare the oxidation mechanisms of methanol and EG and the surface compositions of both catalysts. According to the bifunctional mechanism of the electro-oxidation of methanol [9], CO species adsorbed on platinum sites needs a nearby OH species adsorbed on ruthenium sites in order to complete the oxidation of methanol to the

Table 2
Comparison of various results for homemade and commercial catalysts.

Catalyst	ECSA [$m^2\,g^{-1}$ Pt]	ECSA [$m^2\,g^{-1}$ Pt–Ru]	Particle size [nm]	$I_{0.45}$ for MeOH [A g^{-1} Pt]	$I_{0.45}$ for EG [A g^{-1} Pt]
Homemade Pt/Ru/XC72	42	19	Ru: 5.4 nmPt: 2.7 nm	471	241
Commercial JM	25	16	2.1 nm	346	263

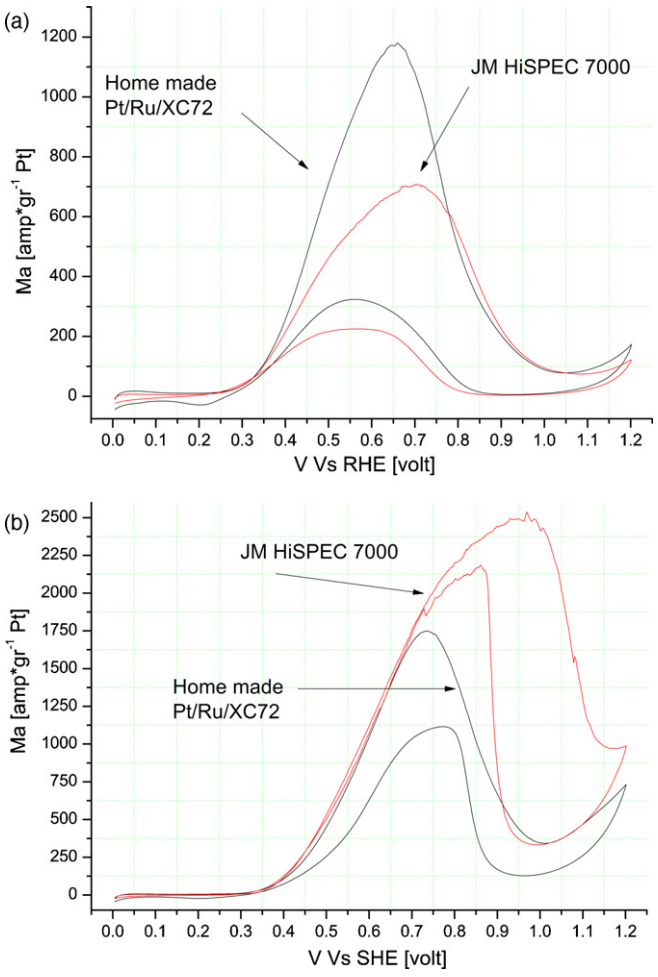

Fig. 3. (a) Typical voltamograms of MeOH oxidation activity in 0.5 M H_2SO_4 + 0.1 M MeOH solution, scan rate: 20 mV s^{-1}. (b) Typical voltammograms of EG oxidation activity in 0.5 M H_2SO_4 + 0.4 M EG solution, scan rate: 20 mV s^{-1}.

final product: CO_2. Obviously, methanol needs one OH species for the process, since it is a single-carbon molecule.

The oxidation process of EG molecule requires a higher number of OH species since it has two carbon atoms. Moreover, some of the transition states during the oxidation might require a participation of additional OH species [27]. Thus, it is likely to assume that an efficient catalyst for EG electro-oxidation might require more Ru sites for every catalytic platinum site than in the case of MeOH electro-oxidation. Support for this assumption can be seen in [28].

A comparison of the XPS analysis of homemade Pt/Ru/XC72 with that of the JM catalyst reveals a large difference in surface composition: a Ru:Pt ratio of 1:4.27 (see Table 1 for the ink sample) and 1:1.6, respectively, i.e., the design of the JM catalyst appears to be much more suited for the EG electro-oxidation mechanism (and methanol oxidation, as was mentioned previously). Unfortunately, the advantage of the Pt/Ru/XC72 catalyst (a highly enriched platinum shell) becomes a great disadvantage when it comes to producing a sufficient number of OH species on ruthenium sites in order to complete the oxidation process of EG. It is very likely that if our catalyst had a surface Ru/Pt composition ratio closer to unity it would have better catalytic activity not only for EG oxidation but for methanol oxidation as well. It should be noted that the problem is not the core–shell structure itself, but that the amount of ruthenium in the shell is too small.

In order to examine the stability of methanol oxidation for both catalysts, chronoamperometric studies were performed as described above.

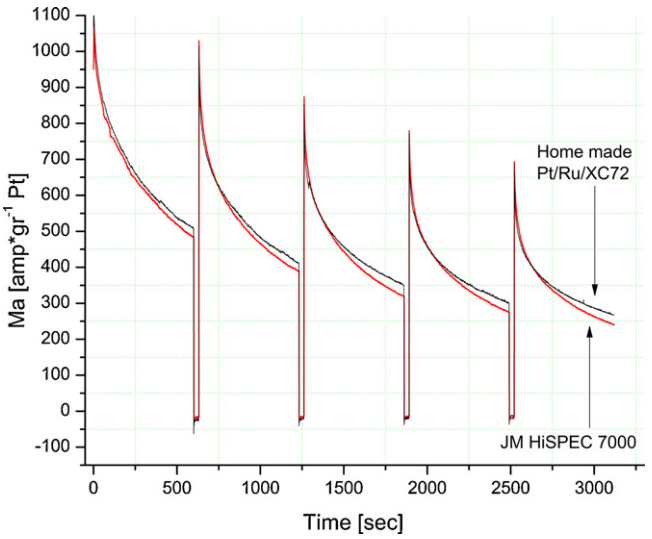

Fig. 4. Chronoamperometric studies of MeOH oxidation stability in 0.5 M H_2SO_4 + 1 M MeOH solution at 0.45 V.

The results of these studies can be seen in Fig. 4. As with methanol oxidation by cyclic voltammetry, the Pt/Ru/XC72 core–shell catalyst shows slightly better results than the commercial JM catalyst. However, after almost 1 h of operation, the advantage of the homemade catalyst diminishes to only 10%. This drastically diminished advantage can be explained by greater cumulative poisoning of the homemade catalyst due to the imbalance in the amount of platinum in the catalyst shell, as explained above. This cumulative poisoning did not occur in the cyclic voltammetry experiment since the surface of the catalyst was "cleaned" during every cycle by oxygen evolution at potentials above 1 V.

The decay with time of the methanol oxidation current is similar for both catalysts, indicating a similar poisoning mechanism by CO. The application of zero volts (on the hydrogen scale) for 30 s on both catalysts caused partial regeneration of their activity. This is explained by the partial cleaning (desorption) of the adsorbed CO species. However, this cleaning process becomes less efficient with time. It is interesting to note that the poisoning and cleaning processes are similar for both catalysts although their surface composition is different.

4. Summary

In this paper we have shown that the deposition of ruthenium on XC72 by a polyol procedure followed by the electroless deposition of platinum with the use of $NaBH_4$, can produce a Pt–Ru-based catalyst, with a distinctive Ru_{core}–Pt_{shell} structure. Catalyst's content was verified by EDS, while the existence of a core–shell structure was confirmed by XPS, TEM and XRD examination. Additionally, XRD provided the size of the catalyst's nanoparticles. Using a CV technique, we have shown that this Ru_{core}–Pt_{shell} catalyst can perform significantly better (up to 36% in our examination) during methanol oxidation at high temperatures, than one of the best commercially available, alloy-based JM catalyst. However, chronoamperometry, which simulates the operation of a real-life DMFC, showed only a moderate improvement in performance.

For ethylene glycol oxidation, this core–shell catalyst did not perform as well as the alloy-based JM catalyst, probably as a result of too-low ruthenium content of the surface.

Although the concept of the Ru_{core}–Pt_{shell} catalyst was proven to be successful, in seeking the goal of enhanced oxidation activity, it needs further optimization of the surface Ru/Pt composition ratio.

References

[1] S.K. Kamarudin, F. Achmad, W.R.W. Daud, Int. J. Hydrogen Energy 34 (2009) 6902–6916.
[2] N. Travitsky, et al., J. Power Sources (2009), doi:10.1016/j.jpowsour.2009.05.025.
[3] V. Livshits, M. Philosoph, E. Peled, J. Power Sources 178 (2) (2008) 687–691.
[4] V. Livshits, E. Peled, J. Power Sources 162 (2) (2006) 1187–1191.
[5] V. Livshits, T. Duvdevani, E. Peled, J. Power Sources 106 (1–2) (2002) 245–248.
[6] T. Duvdevani, A. Aharon, A. Melman, E. Peled, Electrochem. Solid-State Lett. 4 (4) (2001) A38–A41.
[7] H. Wang, Y. Zhao, Z. Jusys, R.J. Behm, J. Power Sources 155 (1) (2006) 33–46.
[8] A. Lewera, W.P. Zhou, C. Vericat, J.H. Chung, R. Haasch, A. Wieckowski, P.S. Bagus, Electrochim. Acta 51 (2006) 3950–3956.
[9] M. Watanabe, S. Motto, J. Electroanal. Chem. 60 (1975) 267.
[10] A.S. Arico, V. Baglio, E. Modica, A. Di Blasi, V. Antonucci, Electrochem. Commun. 6 (2004) 164–169.
[11] A.S. Arico, V. Baglio, E. Modica, A. Di Blasi, G. Monforte, V. Antonucci, J. Electroanal. Chem. 576 (2005) 161–169.
[12] N. Travitsky, T. Ripenbein, D. Golodnitsky, Y. Rosenberg, L. Burshtein, E. Peled, J. Power Sources 161 (2006) 782–789.
[13] G.-Y. Yu, W.-X. Chen, Y.-F. Zheng, J. Zhao, X. Li, Z.-D. Xu, Mater. Lett. 60 (2006) 2453–12453.
[14] JADE 9.1+ Software, Materials Data, Inc., Livermore, CA 94550, USA, 2009.
[15] The International Centre for Diffraction Data (ICDD), 12 Campus Blvd., Newtown Square, PA, 19073-3273, USA, 2009.
[16] The Inorganic Crystal Structure Database (ICSD), FIZ, Karlsruhe 76344, Germany, 2009.
[17] K. Kinoshita, P.N. Ross, J. Electroanal. Chem. 78 (1977) 313.
[18] L. Clare, A. Kucernak, J. Phys. Chem. B 106 (2002) 1036.
[19] M. Goor, M.Sc. Thesis, Tel-Aviv University, September, 2007.
[20] C. Eickes, P. Piela, J. Davey, P. Zelenay, J. Electrochem. Soc. 153 (1) (2006) A171–A178.
[21] A.R. Denton, N.W. Ashcroft, Phys. Rev. A 43 (1991) 3161–3164.
[22] Y. Le Page, C. Bock, J.R. Rodgers, J. Alloys Compd. 422 (2006) 164–172.
[23] B.E. Warren, X-ray Diffraction, Addison-Wesley, Reading, MA, 1969.
[24] S. Alayoglu, P. Zavalij, B. Eichhorn, Q. Wang, A.I. Frenkel, P. Chupas, ACS Nano 10 (2009) 3127–3137.
[25] M.A. Ortigoza, S. Stolbov, T.S. Rahman, Phys. Rev. B 78 (2008) 195417.
[26] M. Philosoph, Ph.D. Thesis, Tel-Aviv University, March, 2009.
[27] G. Horanyi, V. Kazarinov, Y. Vassiliev, V. Andreev, J. Electroanal. Chem. 147 (1983) 263–278.
[28] A.O. Neto, T.R.R. Vasconselos, R.W.R.V. da Silva, M. Linardi, E.V. Spinacé, J. Appl. Electrochem. 35 (2005) 193–198.